Modulation of the B(3)–H→Ru Distances in 7,8-Dicarba-*nido*-undecaborate Derivatives

Francesc Teixidor,*,† José A. Ayllón,† Clara Viñas,† Raikko Kivekäs,‡
Reijo Sillanpää,§ and Jaume Casabó*,∥

Institut de Ciència dels Materials (CSIC), Campus Universitat Autònoma de Barcelona, Bellaterra, 08193 Barcelona, Spain, Departament de Química, Universitat Autònoma de Barcelona, Bellaterra, 08193 Barcelona, Spain, Department of Chemistry, University of Helsinki, P.O. Box 6, FIN-00014, Finland, and Department of Chemistry, University of Turku, FIN-20500 Turku, Finland

Received January 28, 1994®

The formation of B(3)–H→Ru bonds in 7,8-dicarba-*nido*-undecaborate derivatives containing sulfur atoms connected to the cluster carbon atoms is described. The strength of the agostic bond is modulated by modifying the length of the S,S′ connecting chain. Shorter chains (more strained) produce shorter B(3)···Ru distances; longer chains produce longer B(3)···Ru distances. A relationship between the ^{1}H NMR B(3)–*H* hydride or the *B*(3) ^{11}B NMR signals and the external chain has also been disclosed. Two extreme types of B(3)–H→Ru agostic bonds are described. The crystal structures of [RuCl(**L5**)(PPh$_3$)$_2$], [RuCl(**L8**)(PPh$_3$)$_2$]·Me$_2$CO, and [NMe$_4$][RuCl(**L6**)$_2$] are presented. The compound [RuCl(**L5**)(PPh$_3$)$_2$] (M_r = 870.65) crystallizes in the monoclinic space group $P2_1/c$, with a = 15.134(3) Å, b = 11.825(3) Å, c = 22.970(4) Å, α = 90.0°, β = 110.32(2)°, γ = 90.0°, V = 4111(2) Å^3, Z = 4, R = 0.058, and R_w = 0.041. The compound [RuCl(**L8**)(PPh$_3$)$_2$]·Me$_2$CO (M_r = 970.80) crystallizes in the triclinic space group $P\bar{1}$, with a = 12.187(4) Å, b = 17.163(3) Å, c = 8.196(2) Å, α = 95.73(1)°, β = 95.51(2)°, γ = 105.61(2)°, V = 2389(1) Å^3, Z = 2, R = 0.041, and R_w = 0.046. The compound [NMe$_4$][RuCl(**L6**)$_2$] (M_r = 657.84) crystallizes in the orthorhombic space group $Cmc2_1$, with a = 19.423(4) Å, b = 13.028(2) Å, c = 12.142(2) Å, α = 90.0°, β = 90.0°, γ 90.0°, V = 3073(1) Å^3, Z = 4, R = 0.064, and R_w = 0.064.

The incorporation of S,S′-connected chains in the moiety 7,8-dithio-7,8-dicarba-*nido*-undecaborate(1−) is being thoroughly studied in our group.[1] Our results suggest that the length of the chain modulates the B(3)···M distance; e.g., the shorter the chain, the smaller the distance produced. Consequently, short chains should favor B(3)···Ru interactions. This led to the hypothesis that, using short exocluster chains such as SCH$_2$CH$_2$S in **L6** (Table 1), the B(3)–H→M agostic bond could be found for the first time.[2] By using this hypothesis, we had found a B(3)–Rh σ interaction in [N(CH$_3$)$_4$][RhCl{7,8-μ-S(CH$_2$CH$_2$)S-C$_2$B$_9$H$_{10}$}{σ-7,8-μ-S(CH$_2$CH$_2$)S-C$_2$B$_9$H$_9$}].[3]

Three general modes for bonding of the *nido* ion [7,8-C$_2$B$_9$H$_{12}$]$^-$ to M (transition-metal ion) have been reported: η^5 coordination to the open pentagonal C$_2$B$_3$ face[4] as in *closo*-[(PPh$_3$)$_2$RuH$_2$C$_2$B$_9$H$_{11}$],[5] *exo-nido* coordination as in *exo-nido*-[(PPh$_3$)$_2$Rh] [7,8-μ-(CH$_2$)$_3$-7,8-C$_2$B$_9$H$_{10}$],[6] and a mixed mode composed of η^5 coordination and one Rh–H–B bridge as in [Rh(PPh$_3$)C$_2$B$_9$H$_{11}$]$_2$.[7] Besides these three types of M–C$_2$B$_9$ interactions, a more rare M–B σ bond is also known; e.g., a B(10)–Ru σ bond is encountered in [N(PPh$_3$)$_2$][RuW(μ-CC$_6$H$_4$Me-4)(μ-σ,η^5-C$_2$B$_9$H$_8$Me$_2$)(CO)$_3$(η-C$_5$H$_5$)].[8] All B–H→M or B–M bonds found in the literature for derivatives of [7,8-C$_2$B$_9$H$_{12}$]$^-$ involve one

Table 1. *nido*-Carborane Ligands with Their Abbreviations and the Complexes Obtained

Ligands	
{7,8-μ-(SCH$_2$S)-7,8-C$_2$B$_9$H$_{10}$}$^-$ (**L5**)	
{7,8-μ-(SCH$_2$CH$_2$S)-7,8-C$_2$B$_9$H$_{10}$}$^-$ (**L6**)	
{7,8-μ-(SCH$_2$CH$_2$CH$_2$S)-7,8-C$_2$B$_9$H$_{10}$}$^-$ (**L7**)	
{7,8-μ-(SCH$_2$CH$_2$CH$_2$CH$_2$S)-7,8-C$_2$B$_9$H$_{10}$}$^-$ (**L8**)	
{7,8-μ-(SCH$_2$CH$_2$OCH$_2$CH$_2$OCH$_2$CH$_2$S)-7,8-C$_2$B$_9$H$_{10}$}$^-$ (**L12**)	
{7,8-μ-(SCH$_2$CH$_2$OCH$_2$CH$_2$OCH$_2$CH$_2$OCH$_2$CH$_2$S)-7,8-C$_2$B$_9$H$_{10}$}$^-$ (**L15**)	
{7,8-(SCH$_3$)$_2$-7,8-C$_2$B$_9$H$_{10}$}$^-$ (**Lo**)	
Complexes	
[RuCl(**L5**)(PPh$_3$)$_2$]	[RuH(**L7**)(PPh$_3$)$_2$]
[RuCl(**L6**)(PPh$_3$)$_2$]	[RuH(**L8**)(PPh$_3$)$_2$]
[RuCl(**L7**)(PPh$_3$)$_2$]	[RuCl(**L6**)(Me$_2$SO)$_2$]
[RuCl(**L8**)(PPh$_3$)$_2$]	[RuCl(**L7**)(Me$_2$SO)$_2$]
[RuCl(**L6**)(PMePh$_2$)$_2$]	[RuCl(**L6**)(phenan)]
[RuCl(**L7**)(PMePh$_2$)$_2$]	[RuCl(**L7**)(phenan)]
[NMe$_4$][RuCl$_2$(**Lo**)(PMePh$_2$)$_2$]	[NMe$_4$][RuCl(**L6**)$_2$]
[RuH(**L6**)(PPh$_3$)$_2$]	[NMe$_4$][RuCl(**L7**)$_2$]

---

† Institut de Ciència dels Materials, Campus Universitat Autònoma de Barcelona.

‡ University of Helsinki.

§ University of Turku.

∥ Departament de Química, Universitat Autònoma de Barcelona.

® Abstract published in *Advance ACS Abstracts,* May 15, 1994.

(1) (a) Teixidor, F.; Rudolph, R. W. *J. Organomet. Chem.* **1983**, *241*, 301. (b) Viñas, C.; Butler, W. M.; Teixidor, F.; Rudolph, R. W. *Organometallics* **1984**, *3*, 503. (c) Viñas, C.; Butler, W. M.; Teixidor, F.; Rudolph, R. W. *Inorg. Chem.* **1986**, *25*, 4369. (d) Teixidor, F.; Romerosa, A. M.; Rius, J.; Miravitlles, C.; Casabo, J.; Viñas, C.; Sánchez, E. *J. Chem. Soc., Dalton Trans.* **1990**, 525. (e) Teixidor, F.; Viñas, C.; Rius, J.; Miravitlles, C.; Casabó, J. *Inorg. Chem.* **1990**, *29*, 149.

(2) Teixidor, F.; Ayllon, J. A.; Viñas, C.; Kivekäs, R.; Sillanpää, R.; Casabó, J. *J. Chem. Soc., Chem. Commun.* **1992**, 1281.

(3) Teixidor, F.; Romerosa, A.; Viñas, C.; Rius, J.; Miravitlles, C.; Casabó, J. *J. Chem. Soc., Chem. Commun.* **1991**, 192.

(4) Dare, H. F.; Howard, J. A. K.; Pilotti, M. U.; Stone, F. G. A.; Szameitat, J. *J. Chem. Soc., Chem. Commun.* **1989**, 1409.

(5) (a) Jung, C. W.; Hawthorne, M. F. *J. Chem. Soc., Chem. Commun.* **1976**, 257. (b) Jung, C. W.; Hawthorne, M. F. *Inorg. Chem.* **1978**, *17*, 2863.

(6) (a) Long, J. A.; Marder, T. B.; Behnken, P. E.; Hawthorne, M. F. *J. Am. Chem. Soc.* **1984**, *106*, 2979. (b) Knobler, C. B.; Marder, T. B.; Mizusawa, E. A.; Teller, R. G.; Long, J. A.; Hawthorne, M. F. *J. Am. Chem. Soc.* **1984**, *106*, 2990.

(7) Behnken, P. E.; Marder, T. B.; Baker, R. T.; Knobler, C. B.; Thompson, M. R.; Hawthorne, M. F. *J. Am. Chem. Soc.* **1985**, *107*, 932.

(8) Green, M.; Howard, J. A. K.; Jelfs, A. N. de M.; Johnson, O.; Stone, F. G. A. *J. Chem. Soc., Dalton Trans.* **1987**, 73.

0276-7333/94/2313-2751$04.50/0

boron atom of the open pentagonal C_2B_3 face. When *exo-nido* coordination takes place, there are two B–H⇀M interactions, the first with an open face boron atom and the second with a boron atom of the second layer.[9] Recently, the *exo-nido* compound [RuCl($R_2C_2B_9H_{10}$)(PPh$_3$)$_2$] (R = H, Me)[10] has been reported, which contains three B–H⇀Ru bonds involving B(5,6,10), two in the second layer and one in the open face. However, in no case, until our preliminary report on [RuCl(**L6**)(PPh$_3$)$_2$],[2] was there found a B(3)–H⇀M agostic bond. In contrast to the other reported B···M contacts this is unique in the sense that it only involves one boron atom, which is a non open face. Furthermore, this atom is B(3), which is the only boron atom in the cage connected to both carborane carbon atoms, and special properties could be foreseen.

Here we report on such an interaction and, most importantly, on how it can be modulated from a noncoordinating to a coordinating distance in small steps, producing a fine tuning of the B(3)–H⇀M bond's strength. This tuning is achieved by the macrocycle/carborane mutual interaction that permits the otherwise unlikely formation of rare B(3)–M and B(3)–H⇀M interactions.

Results and Discussion

The ligands studied and the abbreviations used are schematically indicated in Table 1. The reaction of the *nido* ligands **L*n*** (*n* = 5–8) with [RuCl$_2$(LB)$_n$] (LB (Lewis base) = Me$_2$SO (dmso), PPh$_3$, 1,10-phenanthroline (phenan), PMePh$_2$)) in ethanol yields orange solids with the stoichiometry [RuCl(**L*n***)(LB)$_2$]. A similar reaction with the open ligand **Lo** (nonconnecting S,S′-string) was conducted with [RuCl$_2$(PMePh$_2$)$_3$] to give [NMe$_4$][RuCl$_2$(**Lo**)(PMePh$_2$)$_2$]. The compounds [RuCl(**L*n***)(phen)] (*n* = 6, 7) were obtained when [RuCl$_2$(dmso)$_4$] was treated with **L*n*** in the presence of phenanthroline, and [RuH(**L*n***)(PPh$_3$)$_2$] (*n* = 6–8) species were separated upon the reaction of [Ru(AcO)H(PPh$_3$)$_3$] with **L*n*** under similar conditions. The negatively charged complexes [RuCl(**L*n***)$_2$]$^-$ (*n* = 6, 7) were obtained upon the reaction of RuCl$_3$ with 2 equiv of [NMe$_4$](**L*n***). Attempts to prepare other compounds with the stoichiometry [RuCl(**L*n***)$_2$]$^-$ were unsuccessful. The full list of the chemicals synthesized is indicated in Table 2. Equation 1 exemplifies these reactions of **L6** and LB = PPh$_3$.

$$[\mathrm{NMe_4}](\mathbf{L6}) + [\mathrm{RuCl_2(PPh_3)_3}] \xrightarrow[\mathrm{N_2}]{\text{ethanol}} [\mathrm{RuCl}(\mathbf{L6})(\mathrm{PPh_3})_2] + \text{other} \quad (1)$$

The stoichiometries indicated are in agreement with elemental analyses and the ^{1}H NMR integrations. The ^{11}B NMR spectra are very reminiscent of those for the respective parent **L*n*** ligands (2:1:2:2:1:1 pattern); however, the first intensity 1 resonance assigned to B(3) has been displaced to higher field in the complexes to usually produce 2:2:2:1:1:1 patterns. The assignment of the B(3) resonance has been confirmed by a heteronuclear correlation (HETCOR) 2D NMR spectrum for [RuCl(**L7**)(PPh$_3$)$_2$], which is presented in Figure 1. The displacement $\Delta\delta$(B(3)) varies considerably from one compound to another; however, it is *upfield* and near 20 ppm for most of the compounds. Table 2 presents the $\Delta\delta$(B(3)) values calculated as

Table 2. Displacement of Chemical Shifts ($\Delta\delta$(B(3))) in ^{11}B NMR and Chemical Shift of H(3) in ^{1}H NMR Resonances

compd	$\Delta\delta$(B(3)) (ppm)	δ(H(3)) (ppm)
[RuCl(**L5**)(PPh$_3$)$_2$]	10	−14.2
[RuCl(**L6**)(PPh$_3$)$_2$]	20	−17.4
[RuCl(**L7**)(PPh$_3$)$_2$]	20	−17.3
[RuCl(**L8**)(PPh$_3$)$_2$]	16	−18.2
[RuCl(**L6**)(PMePh$_2$)$_2$]	20	−17.4
[RuCl(**L7**)(PMePh$_2$)$_2$]	18	−17.1
[NMe$_4$][RuCl$_2$(**Lo**)(PMePh$_2$)$_2$]	1	
[RuH(**L6**)(PPh$_3$)$_2$]	15	−4.3
[RuH(**L7**)(PPh$_3$)$_2$]	10	−3.4
[RuH(**L8**)(PPh$_3$)$_2$]	6	−2.1
[RuCl(**L6**)(Me$_2$SO)$_2$]	20	−14.7
[RuCl(**L7**)(Me$_2$SO)$_2$]	*a*	−14
[RuCl(**L6**)(phenan)]	*a*	
[RuCl(**L7**)(phenan)]	*a*	
[NMe$_4$][RuCl(**L6**)$_2$]	20	−17.5
[NMe$_4$][RuCl(**L7**)$_2$]	13	−7.2

[a] The precise chemical shift was not determinate due to overlap.

$$\Delta\delta(\mathrm{B}(3)) = \delta(\mathrm{B}(3))_{\text{free ligand}} - \delta(\mathrm{B}(3))_{\text{complex}}$$

for the different complexes. Smaller $\Delta\delta$(B(3)) values are found for the hydride series RuH(**L*n***)(PPh$_3$)$_2$ (*n* = 6–8), decreasing from 15 to 6 with the increase in chain length. The longest S,S′ connecting string (*n* = 8) produces the smallest $\Delta\delta$(B(3)) (6 ppm), the medium-size string (*n* = 7) produces an intermediate $\Delta\delta$(B(3)) value (10 ppm), and the shortest string (*n* = 6) produces the largest $\Delta\delta$(B(3)) (15 ppm). Other values outside the 15–20 ppm range are for [RuCl(**L5**)(PPh$_3$)$_2$] (10 ppm) and [NMe$_4$][RuCl(**L7**)$_2$] (13 ppm). Consequently, the statement "*the longer the external chain, the smaller the $\Delta\delta$(B(3)) value*" clearly applies in the hydride series. In fact, it can be extended to all other series described in Table 2. The only compounds which do not strictly follow this rule are those derived from **L5**. According to the literature[11] a *downfield* displacement in the range 5–20 ppm would be expected in three-center–two-electron B–H⇀M interactions; however, this does not correlate with our data. A 25 ppm *upfield* displacement for the B(3) resonance had been proven in [NMe$_4$][RhCl{7,8-μ-S(CH$_2$CH$_2$)S-C$_2$B$_9$H$_{10}$}{σ-7,8-μ-S(CH$_2$CH$_2$)S-C$_2$B$_9$H$_9$}],[3] where a direct B(3)–Rh bond was found. The upfield shift of the B(3) ^{11}B NMR resonance shown by our compounds could be interpreted as these compounds having a B(3)–Ru σ direct bond in solution; however, the HETCOR spectrum (Figure 1) shows that this is not the case, since B(3) is connected to a hydrogen atom. Therefore, the upfield shift of the B(3) ^{11}B NMR resonance has to do simply with the unique nature of B(3) being connected to both carbon atoms in the C$_2$B$_9$ cluster. The gradation of $\Delta\delta$(B(3)) values (Table 2) implies a gradation of Ru–B(3) interactions in the compounds. The largest $\Delta\delta$(B(3)) value would imply more Ru–B(3) σ direct bond contribution to the B(3)–H⇀Ru bond, while the smallest $\Delta\delta$(B(3)) value would imply the largest Ru–H⇀B(3) contribution. The ^{1}H NMR spectra also support the existence of a modulation in the B(3)–H⇀Ru interactions. Resonances near −18 ppm are displayed for almost every compound presented, which are associated with B(3)–*H*⇀Ru. Exceptions to the −18

---

(9) Hewes, J. D.; Kreimendhal, C. W.; Marder, T. B.; Hawthorne, M. F. *J. Am. Chem. Soc.* 1984, *106*, 5757.

(10) Chizhevsky, I. T.; Lobanova, I. A.; Bregadze, V. I.; Petrovskii, P. V.; Antonovich, V. A.; Polyakov, A. V.; Yanovskii, A. I.; Struchkov, Y. T. *Mendeleev Commun.* 1991, 47.

(11) Behnken, P. E.; Marder, T. B.; Baker, R. T.; Knobler, C. B.; Thompson, M. R.; Hawthorne, M. F. *J. Am. Chem. Soc.* 1985, *107*, 932.

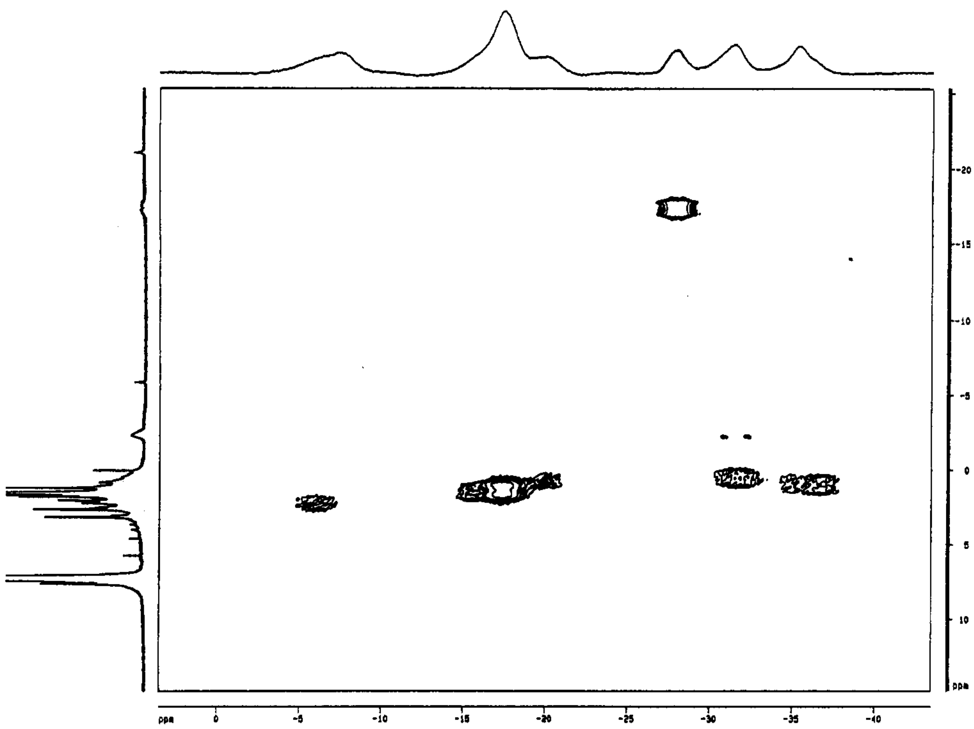

Figure 1. Heteronuclear correlation $^{11}B\{^1H\}$ ^1H 2D NMR of [RuH(**L7**)(PPh$_3$)$_2$].

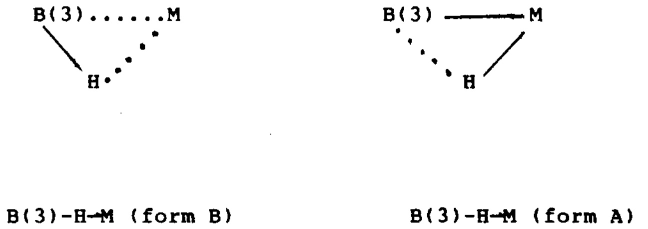

Figure 2. Proposed molecular structures for forms A and B.

ppm value are found in [RuH(**Ln**)(PPh$_3$)$_2$] (n = 6–8) with hydride ^1H NMR resonances at −4.3, −3.4, and −2.1 ppm, respectively, in [RuCl(**Ln**)(dmso)$_2$] (n = 6, 7) (−14.7 and −14.0 ppm, respectively), and in [RuCl(**L5**)(PPh$_3$)$_2$] (−14.2 ppm). This broad field of B(3)–H→M resonances ranging from −2.1 to −18.2 ppm in a series of very similar compounds suggests again that different sorts of B(3)–H→M interactions are present, which tentatively could be depicted as forms A and B (Figure 2). Form B correlates with the low field of the negative site of the ^1H NMR values, while form A correlates with the high field of the negative site of the ^1H NMR values. The specific Ru–H bonds found in the hydride series present this resonance at −21 ppm, which could be dealt with the signal for a non-boron-interacting hydride. In contrast to the ruthenacarborane cluster [RuCl(R$_2$C$_2$B$_9$H$_{10}$)(PPh$_3$)$_2$] mentioned above,[10] only one set of signals has been found in these **Ln**–Ru compounds. The only ^1H NMR spectrum that has presented two sets of signals in the hydride region corresponds to [RuH(**Ln**)(PPh$_3$)$_2$] (n = 6–8). Resonances near −3 and −21 ppm (1:1) are observed in these compounds, which are assigned to B(3)–H→Ru (form B) and Ru–H. Those NMR values can, to a first approximation, tentatively be used as “pure” for the frozen B(3)–H→Ru (form B) and Ru–H, and we can consider the observed chemical shifts for the other Ru complexes as being due to intermediate states between B(3)–H→Ru form B and A representations, respectively. The case for a population-averaged chemical shift under “fast-exchange” conditions has not been considered, since ^1H NMR focused on the signal at −17.4 ppm for [RuCl(**L6**)(PPh$_3$)$_2$] is not resolved at low temperatures (see Figure 3). The ^1H and ^{11}B NMR chemical shift data prove that different sorts of B(3)–H→Ru interactions are possible, depending on the chain length and other coordinating groups present in the molecule.

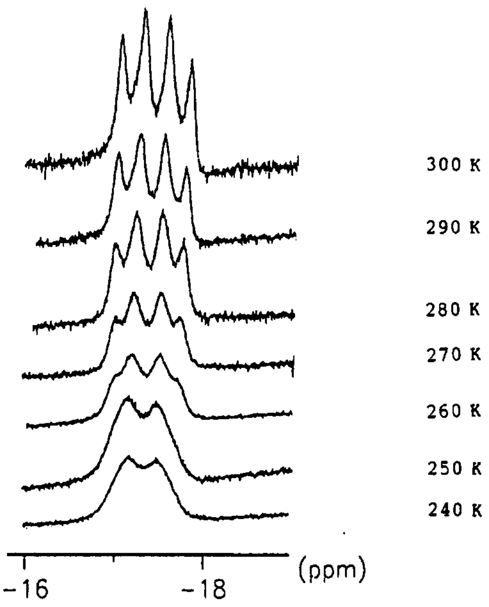

Figure 3. Observed variable-temperature ^1H NMR spectra (400 MHz) for [RuCl(**L6**)(PPh$_3$)$_2$].

The chain's influence on the modulation of the B···M interaction is noteworthy. This will be thoroughly discussed later with the molecular structures reported; however, the ^{11}B and ^1H NMR spectra also provide information on this subject. The ^{11}B NMR of [NMe$_4$][RuCl$_2$(**Lo**)(PMePh$_2$)$_2$] is the only spectrum where $\Delta\delta$(B(3)) has not been produced (see Table 2). Furthermore, the ^1H NMR does not display any signal in the hydride region at a higher field than 2.5 ppm (B–H–B); therefore,

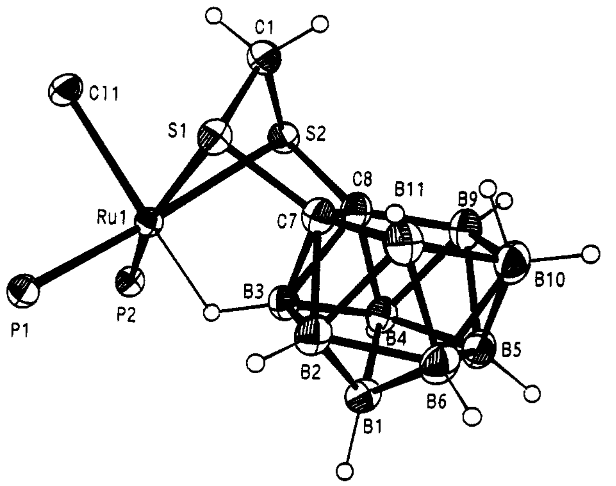

Figure 4. Molecular structure of $[RuCl(\mathbf{L5})(PPh_3)_2]$. Radii are drawn at the 30% level, and H atoms have been omitted.

no B···M interaction is present in this complex. The carborane ligand **Lo**, unlike **L*n***, does not have an outer ring, which is the other factor that we always have considered necessary to force the B···M interaction. As stressed in the Introduction, it is expected that shorter S,S′-connected chains facilitate the B···M interaction. In some ways **Lo** can be thought of as having an infinite S,S′-connecting chain, which is in opposition to the B···M interaction facilitating factor. As a result, there is a gradation of stability of the B···M interaction from zero (**Lo**, open chain) to B(3)–H⇀M forms A and B, depending on the length of the chain. As a result, a way of modulating the B(3)–H⇀M interaction has been made possible.

To provide more information on the B(3)···M modulation capacity of the **L*n*** ligands, the molecular structures of these compounds were clearly determined in the solid state by X-ray diffraction studies. Now, a variation of the B(3)···Ru distance would be expected as a function of the chain's length.

The molecular structures of the complexes $[RuCl(\mathbf{L5})(PPh_3)_2]$ and $[RuCl(\mathbf{L8})(PPh_3)_2]\cdot Me_2CO$ are shown in Figures 4 and 5. The crystal structure of $[RuCl(\mathbf{L6})(PPh_3)_2]\cdot Me_2CO$ has been described previously.[2] Tables 3 and 4 list positional parameters, and Tables 5 and 6 list selected bond lengths and angles. The three molecular structures are very similar, yielding an opportunity to compare S,S′-chain lengths, B(3)···Ru distances, and *w* angles.[19] As indicated, it would be expected that the B(3)–Ru distance would follow the order *d*(B(3)–Ru) in $[RuCl(\mathbf{L5})(PPh_3)_2]$ < *d*(B(3)–Ru) in $[RuCl(\mathbf{L6})(PPh_3)_2]$ < *d*(B(3)–Ru) in $[RuCl(\mathbf{L8})(PPh_3)_2]$. Furthermore, the *w* angle would follow the same trend: *w* angle in $[RuCl(\mathbf{L5})(PPh_3)_2]$ < *w* angle in $[RuCl(\mathbf{L6})(PPh_3)_2]$ < *w* angle in $[RuCl(\mathbf{L8})(PPh_3)_2]$. The molecular structures consist of an octahedral Ru(II) chloride moiety attached to **L5**, **L6**, or **L8** through the sulfur atoms and to two PPh_3 ligands. The carborane ligand is further coordinated to the Ru atom via a B–H⇀Ru agostic bond. As usually found with metal complexes of these 7,8-dicarba-*nido*-undecaborate(1−) derivatives, the metal ion occupies an anti disposition with regard to the open pentagonal C_2B_3 face. Most relevant, however, is the comparison of the *w* angles and the B–Ru distances indicated above. In Table 7, which compares compounds **7**–**9** (equal in all respects but the length S,S′-chain in the carborane ligand), we observe the lengthening of the B(3)–Ru distance from 2.395(5) Å in $[RuCl(\mathbf{L5})(PPh_3)_2]$ to 2.409(5) Å in $[RuCl(\mathbf{L6})(PPh_3)_2]$ to 2.483(4) Å in $[RuCl(\mathbf{L8})(PPh_3)_2]$. Even a larger and gradual increase is found in the *w* angle, ranging from 102.7° in $[RuCl(\mathbf{L5})(PPh_3)_2]$ to 110.0° in $[RuCl(\mathbf{L6})(PPh_3)_2]$ to 120.4° in $[RuCl(\mathbf{L8})(PPh_3)_2]$. The gradation in values observed here is a clear proof of the chain influence on the coordinating ability of these ligands. It is found that fine modulation of the B–H⇀Ru bond (forms A and B) can be made by modifying the length of the chain, enhancing or diminishing the hydride character of the participating H atom. This concept can be of interest in the design of new selective catalysts. As a matter of comparison these B(3)···Ru (B(3)–H⇀Ru) distances (2.48–2.39 Å) are longer than the Ru–B(10) distance (2.15 Å) found in $[N(PPh_3)_2][RuW(\mu\text{-}CC_6H_4Me\text{-}4)(\mu\text{-}\sigma,\eta^5\text{-}C_2B_9H_8Me_2)(CO)_3(\eta\text{-}C_5H_5)]$[8] and longer than the B(3)–Rh distance (2.12 Å) found in $[N(Me_3)_4][RhCl\{7,8\text{-}\mu\text{-}S(CH_2CH_2)S\text{-}C_2B_9H_{10}\}\{\sigma\text{-}7,8\text{-}\mu\text{-}S(CH_2CH_2)S\text{-}C_2B_9H_9\}]$, but they are close to the B(10)···Ru (B(10)–H⇀Ru) distance found (2.40 Å) in $[RuW(\mu\text{-}CC_6H_4Me\text{-}4)(CO)_3(\eta\text{-}C_5H_5)(\eta^5\text{-}C_2B_9H_9Me_2)]$.[8]

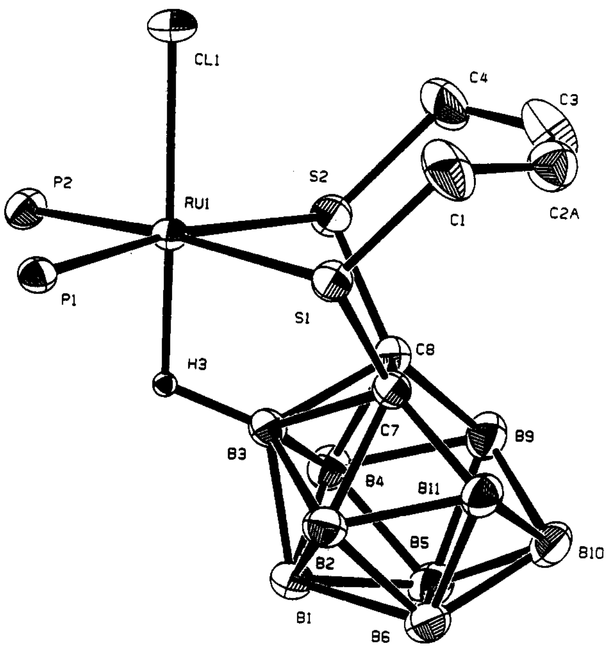

Figure 5. Molecular structure of $[RuCl(\mathbf{L8})(PPh_3)_2]\cdot Me_2CO$. Radii are drawn at the 30% level, and H atoms have been omitted.

The crystal structure of $[NMe_4][RuCl(\mathbf{L6})_2]$ shows that the cages are disordered in such a way that the *nido* cages have two orientations, resulting overall in pseudo *closo* cages. In them, B(3) is situated at two positions, B(3A) and B(3B), with pp = 0.5 for each (pp = population parameter). The Cl and Ru atoms are on the mirror plane and the disordered cages are at both sides of this plane. In a chemical sense this means (see Figure 6) that when there is a boron atom at the position B(3A) there is no boron atom at $B(3A^m)$ but at $B(3B^m)$ (m = symmetry operation for a mirror). Table 8 lists positional parameters, and Table 9 lists selected bond lengths and angles. The molecular structure of $[NMe_4][RuCl(\mathbf{L6})_2]$ consists of a hexacoordinated Ru atom bonded to one Cl and to four sulfur atoms from the two **L6** ligands. Facing the sixth position, which is trans to the Cl, there is a B–H group which forms the agostic bond B(3)–H⇀Ru and a C_2B_3 open face from the second cluster. Consequently, the cluster providing the B–H⇀Ru bond has the open face anti with regard to the metal, which is the usual situation

Table 3. Non-Hydrogen Positional and Isotropic Displacement Parameters for [RuCl(L5)(PPh$_3$)$_2$]

	x	*y*	*z*	U_{eq} (Å^2)
Ru(1)	0.21584(2)	0.16062(3)	0.07589(1)	0.0316(2)
Cl(1)	0.29673(7)	−0.00052(9)	0.04128(5)	0.0481(7)
S(1)	0.13556(7)	0.02974(9)	0.14168(4)	0.0396(6)
S(2)	0.08416(7)	0.08009(9)	0.02804(4)	0.0371(6)
P(1)	0.32597(7)	0.20614(9)	0.14460(5)	0.0382(6)
P(2)	0.25625(7)	0.27855(9)	−0.00097(5)	0.0375(6)
C(1)	0.0934(3)	−0.0404(4)	0.0768(2)	0.043(3)
C(10)	0.3199(3)	0.0969(4)	0.2015(2)	0.041(3)
C(11)	0.2682(3)	0.1160(5)	0.2503(2)	0.059(4)
C(12)	0.2501(4)	0.0311(6)	0.2896(2)	0.066(4)
C(13)	0.2851(4)	−0.0725(6)	0.2826(3)	0.079(5)
C(14)	0.3345(5)	−0.0955(6)	0.2345(3)	0.108(6)
C(15)	0.3515(4)	−0.0109(5)	0.1937(3)	0.088(5)
C(20)	0.3198(3)	0.3360(4)	0.1882(2)	0.045(3)
C(21)	0.3781(3)	0.3482(5)	0.2353(2)	0.068(4)
C(22)	0.3772(4)	0.4446(6)	0.2681(3)	0.086(5)
C(23)	0.3203(4)	0.5307(5)	0.2559(3)	0.082(5)
C(24)	0.2623(4)	0.5215(5)	0.2100(3)	0.074(4)
C(25)	0.2620(3)	0.4230(4)	0.1765(2)	0.055(3)
C(30)	0.4420(3)	0.2136(4)	0.1223(2)	0.043(3)
C(31)	0.4933(4)	0.1211(5)	0.1101(3)	0.062(4)
C(32)	0.5810(3)	0.1300(5)	0.0925(2)	0.070(4)
C(33)	0.6176(4)	0.2333(6)	0.0856(2)	0.070(4)
C(34)	0.5687(4)	0.3273(6)	0.0962(3)	0.086(5)
C(35)	0.4813(4)	0.3184(5)	0.1147(2)	0.066(4)
C(40)	0.2578(3)	0.4295(3)	0.0174(2)	0.040(3)
C(41)	0.1825(3)	0.4877(4)	0.0330(2)	0.052(3)
C(42)	0.1859(5)	0.6010(5)	0.0496(2)	0.067(4)
C(43)	0.2652(5)	0.6550(5)	0.0521(3)	0.078(4)
C(44)	0.3399(5)	0.5988(6)	0.0376(3)	0.084(5)
C(45)	0.3380(4)	0.4868(5)	0.0205(2)	0.059(3)
C(50)	0.3585(3)	0.2633(4)	−0.0423(2)	0.042(3)
C(51)	0.3677(3)	0.3283(5)	−0.0929(2)	0.059(3)
C(52)	0.4410(4)	0.3188(5)	−0.1279(2)	0.068(4)
C(53)	0.5052(4)	0.2427(5)	−0.1140(3)	0.070(4)
C(54)	0.4986(3)	0.1777(5)	−0.0646(3)	0.062(4)
C(55)	0.4249(3)	0.1887(4)	−0.0293(2)	0.050(3)
C(60)	0.1791(3)	0.2602(4)	−0.0618(2)	0.039(2)
C(61)	0.1862(3)	0.1596(5)	−0.0931(2)	0.051(3)
C(62)	0.1329(4)	0.1380(5)	−0.1409(2)	0.063(4)
C(63)	0.0700(4)	0.2140(6)	−0.1575(2)	0.067(4)
C(64)	0.0609(3)	0.3135(5)	−0.1281(2)	0.066(4)
C(65)	0.1156(3)	0.3362(5)	−0.0806(2)	0.052(3)
B(1)	0.0140(3)	0.3560(5)	0.1366(2)	0.047(3)
B(2)	0.0531(3)	0.2488(5)	0.1846(2)	0.046(3)
B(3)	0.0854(3)	0.2517(4)	0.1111(2)	0.037(3)
B(4)	−0.0049(3)	0.2965(4)	0.0678(2)	0.041(3)
B(5)	−0.0965(3)	0.3163(5)	0.1139(2)	0.049(3)
B(6)	−0.0582(4)	0.2858(5)	0.1875(2)	0.054(4)
C(7)	0.0458(2)	0.1289(3)	0.1432(2)	0.039(2)
C(8)	0.0142(2)	0.1555(4)	0.0779(2)	0.040(2)
B(9)	−0.0891(3)	0.1871(5)	0.0742(2)	0.048(3)
B(10)	−0.1278(4)	0.1901(5)	0.1501(2)	0.053(4)
B(11)	−0.0306(3)	0.1406(5)	0.1908(2)	0.050(3)

Table 4. Non-Hydrogen Positional and Isotropic Displacement Parameters for [RuCl(L8)(PPh$_3$)$_2$]·Me$_2$CO

atom[a]	*x*	*y*	*z*	*B*(eq) (Å^2)
Ru(1)	0.07625(2)	0.31957(1)	0.28999(2)	2.140(8)
Cl(1)	0.16154(8)	0.44189(5)	0.41880(7)	3.52(3)
S(1)	0.04187(7)	0.39081(5)	0.13239(7)	2.80(3)
S(2)	−0.11615(7)	0.32312(6)	0.32036(7)	3.01(3)
P(1)	0.25384(7)	0.31883(5)	0.22529(7)	2.53(3)
P(2)	0.08038(8)	0.23602(5)	0.43505(7)	2.88(3)
O(1)^{I}	0.472(2)	0.106(1)	0.686(2)	9.3(6)
O(2)^{I}	0.520(1)	−0.035(1)	0.763(1)	6.3(5)
C(1)	0.0120(4)	0.4887(2)	0.1604(5)	5.6(2)
C(2A)^{II}	−0.1027(6)	0.4944(4)	0.1653(6)	4.4(1)
C(2B)^{III}	−0.051(1)	0.513(1)	0.252(1)	6.0(3)
C(3)	−0.1724(5)	0.4653(3)	0.2562(5)	7.1(3)
C(4)	−0.1437(5)	0.4215(3)	0.3497(4)	6.5(2)
C(7)	−0.0918(3)	0.3171(2)	0.0838(3)	2.6(1)
C(8)	−0.1702(3)	0.2846(2)	0.1767(3)	2.7(1)
C(11)	0.2993(3)	0.4047(2)	0.1429(3)	3.0(1)
C(12)	0.3118(3)	0.3934(2)	0.0299(3)	4.0(1)
C(13)	0.3438(4)	0.4607(3)	−0.0293(4)	5.4(2)
C(14)	0.3615(4)	0.5384(3)	0.0239(5)	5.4(2)
C(15)	0.3465(3)	0.5504(2)	0.1351(4)	4.5(2)
C(16)	0.3145(3)	0.4845(2)	0.1946(3)	3.6(1)
C(21)	0.3844(3)	0.3308(2)	0.3250(3)	3.0(1)
C(22)	0.4619(3)	0.4057(2)	0.3657(4)	4.3(2)
C(23)	0.5584(4)	0.4111(3)	0.4413(4)	5.3(2)
C(24)	0.5785(4)	0.3426(3)	0.4750(4)	5.7(2)
C(25)	0.5030(4)	0.2676(3)	0.4350(4)	5.4(2)
C(26)	0.4065(3)	0.2617(2)	0.3603(3)	4.0(1)
C(31)	0.2617(3)	0.2298(2)	0.1319(3)	2.9(1)
C(32)	0.3644(3)	0.2293(2)	0.0898(3)	3.6(1)
C(33)	0.3747(3)	0.1613(3)	0.0252(4)	4.3(2)
C(34)	0.2832(4)	0.0921(2)	0.0019(4)	4.5(2)
C(35)	0.1817(3)	0.0908(2)	0.0418(4)	4.5(2)
C(36)	0.1710(3)	0.1593(2)	0.1071(3)	3.5(1)
C(41)	0.1885(3)	0.2626(2)	0.5605(3)	3.6(1)
C(42)	0.2852(3)	0.3285(2)	0.5745(3)	4.0(1)
C(43)	0.3639(4)	0.3430(3)	0.6717(3)	5.0(2)
C(44)	0.3464(4)	0.2931(3)	0.7536(4)	5.7(2)
C(45)	0.2492(5)	0.2289(3)	0.7429(4)	6.3(2)
C(46)	0.1708(4)	0.2136(3)	0.6470(4)	5.5(2)
C(51)	−0.0471(3)	0.2271(2)	0.5085(3)	3.4(1)
C(52)	−0.1399(4)	0.1595(2)	0.4988(3)	4.2(2)
C(53)	−0.2355(4)	0.1617(3)	0.5533(4)	5.4(2)
C(54)	−0.2364(4)	0.2320(3)	0.6177(4)	5.2(2)
C(55)	−0.1448(4)	0.2993(3)	0.6287(3)	5.2(2)
C(56)	−0.0513(4)	0.2977(3)	0.5747(3)	4.4(2)
C(61)	0.0794(3)	0.1315(2)	0.3844(3)	3.4(1)
C(62)	0.1716(4)	0.1018(3)	0.4153(4)	4.8(2)
C(63)	0.1737(5)	0.0247(3)	0.3676(5)	6.4(2)
C(64)	0.0847(5)	−0.0234(3)	0.2922(5)	6.3(2)
C(65)	−0.0077(4)	0.0043(2)	0.2617(4)	5.3(2)
C(66)	−0.0105(4)	0.0815(2)	0.3072(3)	4.0(1)
C(67)	0.422(1)	0.039(1)	0.703(1)	19.0(5)
C(68)	0.494(2)	−0.012(1)	0.685(2)	21.6(6)
C(69)^{I}	0.318(2)	0.014(1)	0.700(1)	11.0(5)
C(70)^{I}	0.488(2)	0.007(1)	0.577(2)	13.1(5)
B(1)	−0.1557(4)	0.1498(2)	0.0415(4)	3.3(1)
B(2)	−0.0703(4)	0.2378(2)	−0.0055(3)	3.2(1)
B(3)	−0.0736(3)	0.2326(2)	0.1404(3)	2.5(1)
B(4)	−0.2144(3)	0.1793(2)	0.1612(4)	3.2(1)
B(5)	−0.3011(4)	0.1578(3)	0.0314(4)	3.8(2)
B(6)	−0.2096(4)	0.1944(3)	−0.0735(4)	3.5(1)
B(9)	−0.3033(4)	0.2443(3)	0.1253(4)	3.5(2)
B(10)	−0.3081(4)	0.2468(3)	−0.0290(4)	3.9(2)
B(11)	−0.1596(4)	0.3021(3)	−0.0413(4)	3.4(1)

[a] Legend: I, pp (population parameter) = 0.5; II, pp = 0.65; III, pp = 0.35.

in this type of chemistry. The other cluster, however, presents a syn disposition of the open face vs the metal. This is quite abnormal, even with complexes containing two ligands. We consider that the steric repulsions result in a syn disposition of the cage vs the chlorine atom, favoring the disposition found in the crystal structure. It is worth noticing that here the *w* angle in this complex is in the range for the other complexes (see Table 7); however, the distance B–Ru is much greater. This means that a strict correlation between *w* angle and distance is not fully followed, due to a variation in the dihedral angle between C$_2$S$_2$ and C$_2$B$_3$ planes in the complexes with different stoichiometries. The reasons for the variation in this dihedral angle are probably steric in origin.

In conclusion, we have proved the feasibility of the B(3)···M interaction in 7,8-dicarba-*nido*-undecaborate derivatives; this B(3)–H→M interaction can be modulated by modifying the length of an external chain, connected to the carbon atoms of the cluster. The characteristics of this B(3)–H→M interaction are related to the unique nature of B(3), being the only boron atom in the cluster connected to both cluster carbon atoms. The B(3)–H→M modulation is observed in either ^{1}H NMR or in ^{11}B NMR spectroscopy, and a great dispersion of resonance positions for the implicated *B(3)* and B(3)–*H* in related compounds

Table 5. Selected Distances (Å) and Angles (deg) with Esd's in Parentheses for $[RuCl(\mathbf{L5})(PPh_3)_2]$

Ru(1)–Cl(1)	2.403(1)	Ru(1)–B(3)	2.483(4)
Ru(1)–S(2)	2.461(1)	Ru(1)–S(1)	2.486(1)
Ru(1)–P(2)	2.335(1)	Ru(1)–P(1)	2.350(1)
S(1)–C(1)	1.817(4)	Ru(1)–H(503)	1.62(3)
S(2)–C(1)	1.816(4)	S(1)–C(7)	1.795(4)
C(7)–B(2)	1.710(7)	S(2)–C(8)	1.801(4)
C(7)–B(3)	1.7317(6)	B(1)–B(2)	1.777(7)
C(7)–B(11)	1.602(6)	B(1)–B(3)	1.743(7)
C(8)–B(3)	1.739(6)	B(1)–B(4)	1.752(7)
C(8)–B(4)	1.708(7)	B(1)–B(5)	1.811(7)
C(8)–B(9)	1.609(6)	B(1)–B(6)	1.808(8)
B(2)–B(6)	1.741(7)	B(2)–B(3)	1.761(7)
B(3)–B(4)	1.766(7)	B(2)–B(11)	1.807(8)
B(4)–B(9)	1.823(7)	B(4)–B(5)	1.766(7)
B(5)–B(9)	1.782(8)	B(5)–B(6)	1.821(7)
B(6)–B(10)	1.764(8)	B(5)–B(10)	1.774(8)
B(9)–B(10)	1.845(8)	B(6)–B(11)	1.768(8)
C(7)–C(8)	1.603(5)	B(10)–B(11)	1.833(8)

Cl(1)–Ru(1)–S(1)	87.69(4)	P(1)–Ru(1)–H(503)	91(1)
Cl(1)–Ru(1)–S(2)	87.61(4)	P(2)–Ru(1)–H(503)	83(1)
Cl(1)–Ru(1)–P(1)	92.48(4)	Ru(1)–S(1)–C(1)	87.5(1)
Cl(1)–Ru(1)–P(2)	94.97(4)	Ru(1)–S(1)–C(7)	88.8(1)
Cl(1)–Ru(1)–H(503)	176(1)	Ru(1)–S(2)–C(1)	88.3(1)
S(1)–Ru(1)–S(2)	68.46(4)	Ru(1)–S(2)–C(8)	90.2(1)
S(1)–Ru(1)–P(1)	94.69(4)	Ru(1)–P(1)–C(10)	106.1(1)
S(1)–Ru(1)–P(2)	164.41(3)	Ru(1)–P(1)–C(20)	121.3(1)
S(1)–Ru(1)–H(503)	93(1)	Ru(1)–P(1)–C(30)	119.9(1)
S(2)–Ru(1)–P(1)	163.13(4)	Ru(1)–P(2)–C(40)	114.2(1)
S(2)–Ru(1)–P(2)	96.26(4)	Ru(1)–P(2)–C(50)	124.1(1)
S(2)–Ru(1)–H(503)	89(1)	Ru(1)–P(2)–C(60)	109.8(1)
P(1)–Ru(1)–P(2)	100.53(4)		

Table 6. Selected Distances (Å) and Angles (deg) with Esd's in Parentheses for $[RuCl(\mathbf{L8})(PPh_3)_2]\cdot Me_2CO$

Ru(1)–Cl(1)	2.398(1)	Ru(1)–S(1)	2.4174(9)
Ru(1)–S(2)	2.423(1)	Ru(1)–P(1)	2.372(1)
Ru(1)–P(2)	2.370(1)	Ru(1)–B(3)	2.483(4)
Ru(1)–H(3)	1.73(3)	S(1)–C(1)	1.819(4)
S(1)–C(7)	1.776(3)	S(2)–C(4)	1.816(5)
S(2)–C(8)	1.780(3)	O(1)–C(67)	1.19(2)
O(2)–C(68)	1.10(2)	C(7)–B(2)	1.741(5)
B(1)–B(2)	1.766(6)	C(7)–B(3)	1.721(5)
B(1)–B(3)	1.761(5)	C(7)–B(11)	1.605(5)
B(1)–B(4)	1.756(6)	C(8)–B(3)	1.721(5)
B(1)–B(5)	1.807(6)	C(8)–B(4)	1.726(5)
B(1)–B(6)	1.799(6)	C(8)–B(9)	1.616(5)
B(2)–B(3)	1.768(5)	B(2)–B(6)	1.743(6)
B(2)–B(11)	1.800(6)	B(3)–B(4)	1.768(5)
B(4)–B(5)	1.745(6)	B(4)–B(9)	1.805(6)
B(5)–B(6)	1.811(7)	B(5)–B(9)	1.782(6)
B(5)–B(10)	1.775(6)	B(6)–B(10)	1.773(7)
B(6)–B(11)	1.773(6)	B(9)–B(10)	1.856(7)
B(10)–B(11)	1.830(6)	C(7)–C(8)	1.586(5)

Cl(1)–Ru(1)–S(1)	94.42(4)	P(1)–Ru(1)–B(3)	105.28(9)
Cl(1)–Ru(1)–S(2)	92.07(4)	P(2)–Ru(1)–B(3)	104.29(9)
Cl(1)–Ru(1)–P(1)	92.81(4)	Ru(1)–S(1)–C(1)	118.6(2)
Cl(1)–Ru(1)–P(2)	92.13(4)	Ru(1)–S(1)–C(7)	92.0(1)
Cl(1)–Ru(1)–B(3)	153.08(9)	Ru(1)–S(2)–C(4)	118.8(2)
S(1)–Ru(1)–S(2)	83.15(4)	Ru(1)–S(2)–C(8)	91.8(1)
S(1)–Ru(1)–P(1)	87.08(4)	Ru(1)–P(1)–C(11)	109.3(1)
S(1)–Ru(1)–P(2)	170.97(3)	Ru(1)–P(1)–C(21)	121.4(1)
S(1)–Ru(1)–B(3)	67.36(9)	Ru(1)–P(1)–C(31)	119.0(1)
S(2)–Ru(1)–P(1)	169.38(3)	Ru(1)–P(2)–C(41)	124.3(1)
S(2)–Ru(1)–P(2)	90.42(4)	Ru(1)–P(2)–C(51)	110.0(1)
S(2)–Ru(1)–B(3)	67.05(9)	Ru(1)–P(2)–C(61)	113.9(1)
P(1)–Ru(1)–P(2)	98.81(4)		

is found; this modulation is clearly appreciated by studying the B(3)···M length in a series of related compounds. Two extreme types of B(3)–H⇀M interactions are postulated, which are represented in Figure 2 and have been named form A and form B. All sorts of intermediate dispositions are encountered. As a first approximation we have postulated that form B gives ^{1}H NMR δ values of the B(3)–*H*⇀M resonance near −4 ppm while form A has ^{1}H NMR δ values for the same resonance near −18 ppm. Short *exo* cluster chains produce mostly form A, represented in general by high-field *B(3)* ^{11}B NMR and B(3)–*H* ^{1}H NMR resonances and shorter B(3)···M distances in related compounds, in contrast, longer *exo* cluster chains produce mostly form B, represented in general by low-field *B(3)* ^{11}B NMR and B(3)–*H* ^{1}H NMR resonances and longer B(3)···M distances. At the extreme, very long (or open-chain) ligands do not produce the B(3)–H⇀M interactions. In addition, the series of structures and stoichiometries presented in this paper are easily interpreted if they are considered made up of components. The main component is a "common unit" (see Figure 7) which has no charge. If we consider that each Ru has six coordinating sites, two are missing in this common unit. In the case of a neutral "external" ligand (Me_2SO, PPh_3, $PMePh_2$) the structure made up of the common unit and two of those ligands is obtained. In the case of **L6** as the external ligand the same considerations are valid. Consequently, and in contrast to the case where L6 is part of the common unit, the external ligand will only be bidentate; therefore, even though there are two L6's, only one B–H⇀Ru interaction will be found in the resulting complex. Moreover, since the external ligands have to provide zero charge, a tetramethylammonium ion is expected.

Table 7. List of w Angles and B(3)–M and S–S Distances

compd. no.	chain size	*w* (deg)	B(3)–M (Å)	S–S (Å)
1	15	156.8	3.55	3.23
2	12	154.2	3.55	3.22
3	6	131.0	3.27	2.97
4	6	129.4	3.30	2.96
5	6	117.3	2.58	2.96
6	6	108.0	2.12	2.97
7	8	120.4	2.48	3.21
8	6	110.0	2.41	3.01
9	5	102.7	2.39	2.78

1: $[Pd(\mathbf{L15})_2]$
2: $[Rh(\mathbf{L12})(PPh_3)_2]$
3: $[PdCl(\mathbf{L6})(PPh_3)]$
4: $[Rh(\mathbf{L6})(PPh_3)_2]$
5: $[NMe_4][RuCl(\mathbf{L6})_2]$
6: $[NMe_4][RhCl(\mathbf{L6})(\sigma\text{-}\mathbf{L6})]$
7: $[RuCl(\mathbf{L8})(PPh_3)_2]$
8: $[RuCl(\mathbf{L6})(PPh_3)_2]$
9: $[RuCl(\mathbf{L5})(PPh_3)_2]$

Experimental Section

Instrumentation. Elemental analysis were performed in our analytical laboratory using a Perkin-Elmer 240-B microanalyser. IR spectra were obtained with KBr pellets on a Nicolet 710-FT spectrophotometer. The ^{1}H NMR, ^{11}B NMR, and ^{31}P NMR spectra were obtained by using a Bruker AM 400WB instrument. Unless mentioned elsewhere, all preparations were carried out under a dinitrogen atmosphere.

Materials. Before use, *o*-carborane (Dexsil Chemical Corp.) was sublimed under high vacuum; **L5**, **L6**, **L7**, and **L8** were prepared from *o*-carborane according to the literature.[12] A 1.7 M solution of *n*-butyllithium in hexane from Fluka was used as purchased. $[RuCl_2(PPh_3)_3]$, $[RuCl_2(PPh_2Me)_3]$, $[RuCl_2(Me_2SO)_4]$,

---

[12] (a) Teixidor, F.; Rudolph, R. W. *J. Organomet. Chem.* **1983**, *241*, 301. (b) Viñas, C.; Butler, W. M.; Teixidor, F.; Rudolph, R. W. *Organometallics* **1984**, *3*, 503. (c) Viñas, C.; Butler, W. M.; Teixidor, F.; Rudolph, R. W. *Inorg. Chem.* **1986**, *25*, 4369. (d) Teixidor, F.; Rius, J.; Romerosa, A. M.; Miravitlles, C.; Escriche, Ll.; Sanchez, E.; Viñas, C.; Casabó, J. *Inorg. Chim. Acta* **1990**, *176*, 287. (e) Teixidor, F.; Romerosa, A. M.; Rius, J.; Miravitlles, C.; Casabó, J.; Viñas, C.; Sanchez, E. *J. Chem. Soc., Dalton Trans.* **1990**, 525. (f) Teixidor, F.; Viñas, C.; Rius, J.; Miravitlles, C.; Casabó, J. *Inorg. Chem.* **1990**, *29*, 149.

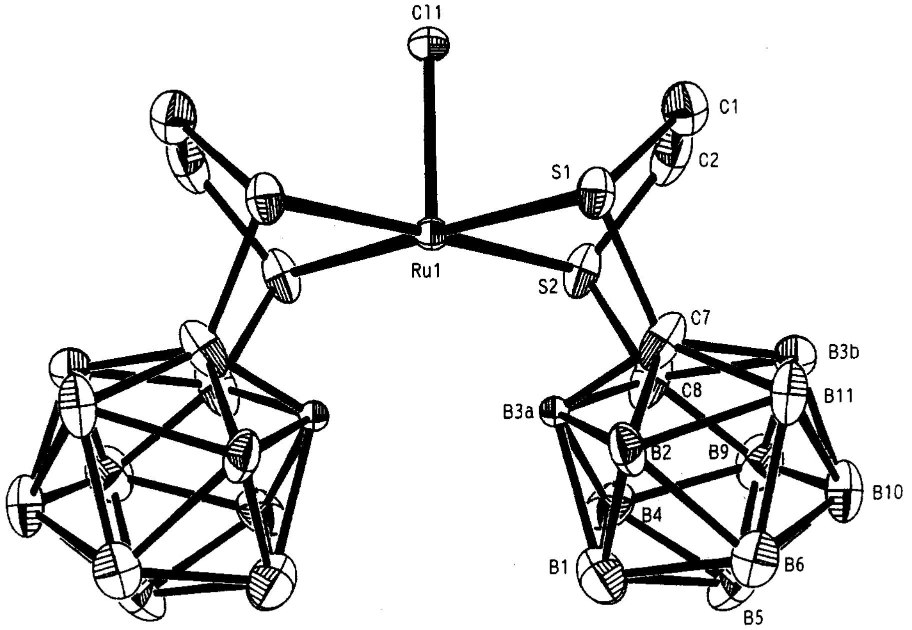

Figure 6. Molecular structure of $[NMe_4][RuCl(L6)_2]$. Radii are drawn at the 30% level, and H atoms have been omitted.

Table 8. Non-Hydrogen Positional and Isotropic Displacement Parameters for $[NMe_4][RuCl(L6)_2]$

atom[a]	*x*	*y*	*z*	U_{eq} (Å^2)
Ru(1)	0	0.37806(9)	0.30000^{IV}	0.0274(3)
Cl(1)	0	0.5198(3)	0.1765(4)	0.043(1)
S(1)	0.0951(2)	0.4461(3)	0.3986(3)	0.041(1)
S(2)	0.0942(2)	0.3072(3)	0.2063(3)	0.047(1)
C(1)	0.1518(6)	0.487(1)	0.286(1)	0.055(5)
C(2)	0.1497(8)	0.414(1)	0.187(1)	0.074(6)
B(1)	0.0956(8)	0.134(1)	0.504(2)	0.065(6)
B(2)	0.1081(7)	0.269(1)	0.545(1)	0.047(5)
B(3A)^{V}	0.071(1)	0.250(2)	0.411(2)	0.021(5)
B(3B)^{V}	0.215(1)	0.285(2)	0.378(2)	0.042(7)
B(4)	0.1062(9)	0.133(1)	0.355(1)	0.060(6)
B(5)	0.1772(9)	0.094(1)	0.443(2)	0.065(7)
B(6)	0.1802(8)	0.173(1)	0.559(2)	0.060(6)
C(7)	0.1329(7)	0.321(1)	0.429(1)	0.050(5)
C(8)	0.1317(6)	0.245(1)	0.324(1)	0.057(5)
B(9)	0.1993(8)	0.162(1)	0.327(1)	0.065(7)
B(10)	0.2391(7)	0.188(1)	0.456(1)	0.055(6)
B(11)	0.2004(8)	0.304(1)	0.512(1)	0.057(6)
N(20)	$^1/_2$	0.305(1)	0.389(1)	0.061(7)
C(21)	$^1/_2$	0.370(2)	0.491(3)	0.12(1)
C(22)	$^1/_2$	0.193(2)	0.412(3)	0.11(1)
C(23)	0.450(1)	0.333(3)	0.326(4)	0.28(2)

[a] Legend: IV, *z* coordinate was fixed; V, population parameter 0.5

Table 9. Selected Distances (Å) and Angles (deg) with Esd's in Parentheses for $[NMe_4][RuCl(L6)_2]$

Ru(1)–Cl(1)	2.379(5)	Ru(1)–S(1)	2.373(3)
Ru(1)–S(2)	2.343(4)	Ru(1)–B(3A)	2.55(2)
S(1)–C(1)	1.84(2)	S(2)–C(2)	1.77(2)
C(1)–C(2)	1.53(2)	S(2)–C(8)	1.80(1)
S(1)–C(7)	1.83(1)	C(7)–B(2)	1.63(2)
B(1)–B(2)	1.84(2)	C(7)–B(3A)	1.53(3)
C(7)–B(3B)	1.76(3)	B(1)–B(3A)	1.95(3)
C(7)–B(11)	1.67(2)	B(1)–B(4)	1.83(3)
C(8)–B(3A)	1.59(3)	C(8)–B(3B)	1.81(3)
B(1)–B(5)	1.83(2)	C(8)–B(4)	1.58(2)
B(1)–B(6)	1.84(2)	C(8)–B(9)	1.70(2)
B(2)–B(3A)	1.79(3)	B(2)–B(6)	1.88(2)
B(2)–B(11)	1.89(2)	B(3A)–B(4)	1.80(3)
B(4)–B(5)	1.82(2)	B(4)–B(9)	1.88(2)
B(5)–B(6)	1.74(3)	B(5)–B(9)	1.71(3)
B(5)–B(10)	1.73(2)	B(6)–B(10)	1.71(2)
B(6)–B(11)	1.84(2)	B(9)–B(10)	1.78(2)
B(10)–B(11)	1.81(2)	C(7)–C(8)	1.61(2)
Cl(1)–Ru(1)–S(1)	91.6(1)	S(2)–Ru(1)–B(3A)	65.0(5)
Cl(1)–Ru(1)–S(2)	90.0(1)	S(2)–Ru(1)–S(2)^{i}	102.6(1)
Cl(1)–Ru(1)–B(3A)	147.4(5)	Ru(1)–S(1)–C(1)	101.5(5)
S(1)–Ru(1)–S(2)	77.6(1)	Ru(1)–S(1)–(7)	94.6(5)
S(1)–Ru(1)–B(3A)	63.8(5)	Ru(1)–S(2)–C(2)	103.3(6)
S(1)–Ru(1)–S(1)^{i}	102.2(1)	Ru(1)–S(2)–C(8)	96.2(4)
S(1)–Ru(1)–S(2)^{i}	178.4(1)		

[a] Legend: i, equivalent position –*x*, *y*, *z*.

and $[Ru(AcO)H(PPh_3)_3]$ were synthesized according to the literature.[13] Ethanol was reagent grade.

Synthesis of $[NMe_4]$Lo. To 40 cm^3 of deoxygenated ethanol containing 350 mg (0.006 mmol) of KOH was added 1,2-dithiol-*o*-carborane (500 mg, 0.002 mmol). After $(CH_3)_2SO_4$ (0.9 g, 7.1 mmol) was added, the mixture was stirred at room temperature for 0.5 h and at reflux for 2 h. Insolubles were separated by filtering the warm mixture. After addition of potassium hydroxide (1.6 g, 28.5 mmol) to the ethanol solution, this mixture was refluxed for 1 h. After evaporation of the solvent, water was added. Tetramethylammonium chloride (excess) was added to the aqueous solution, resulting in the formation of a white precipitate. This was filtered off, washed with water and ether, and dried under vacuum to yield the analytically pure solid $[NMe_4]$Lo, yield 611 mg (85%). FTIR (KBr; ν, cm^{-1}): 2580, 2535 (B–H). ^{1}H FTNMR (400 MHz, CD_3COCD_3, 25 °C, TMS; δ): –2.5 (br, 1, B*H*B), 2.18 (s, 6, C*H*$_3$), 3.45 (s, 12, N(C*H*$_3$)$_4$). ^{11}B FTNMR (128 MHz, CH_3COCH_3, 25 °C, $BF_3\cdot Et_2O$; δ): –8.2 (d, ^1J(B,H) = 140 Hz, 2B), –13.7 (d, ^1J(B,H) = 160 Hz, 1B), –17.6

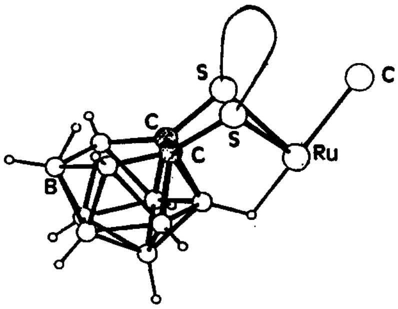

Figure 7. "Common unit".

---

(13) (a) Hallmam, P. S.; Stephenson, T. A.; Wilkinson, G. *Inorg. Synth.* *12*, 237. (b) Chappel, S. D.; Cole Hamilton, D. J.; Galas, A. M. R.; Hursthouse, M. B. *J. Chem. Soc., Dalton Trans.* **1982**, 1867. (c) Mitchel, R. W.; Spencer, A.; Wilkinson, G. *J. Chem. Soc., Dalton Trans.* **1973**, 846. (d) Evans, I. P.; Spencer, A.; Wilkinson, G. *J. Chem. Soc., Dalton Trans.* **1973**, 204.

(d, ^1J(B,H) = 153 Hz, 2B), −19.3 (d, ^1J(B,H) = 163 Hz, 2B), −35.2 (1B), −36.5 (d, ^1J(B,H) = 147 Hz, 1B). Anal. Calcd for $C_8H_{28}B_9NS_2$: C, 32.06; H, 9.42; N, 4.67; S, 21.39. Found: C, 32.02; H, 9.55; N, 4.67; S, 19.77.

Synthesis of [RuCl(L5)(PPh_3)$_2$]. To 30 cm^3 of deoxygenated ethanol containing 30 mg (0.106 mmol) of [NMe_4[(**L5**) was added [$RuCl_2(PPh_3)_3$] (100 mg, 0.104 mmol), and the mixture was refluxed for 1 h. An orange solid was separated by filtering the warm mixture. The solid was washed with warm ethanol and ethyl ether to yield the analytically pure solid [RuCl(**L5**)(PPh_3)$_2$], yield 77 mg (85%). FTIR (KBr; ν, cm^{-1}): 2580, 2558, 2545, 2534 (B–H). ^{1}H FTNMR (400 MHz, $CDCl_3$, 25 °C, TMS; δ): −14.2 (q, 1, Ru*H*), −1.9 (br, 1, B*H*B), 5.59 (d, ^1J = 9.5 Hz, 1, C*H*$_2$), 6.12 (d, ^1J = 9.5 Hz, 1, C*H*$_2$), 7.20–7.44 (m, 30, C_{aryl}–*H*). ^{11}B FTNMR (128 MHz, CH_2Cl_2, 25 °C, $BF_3 \cdot Et_2O$; δ): −5.8 (2B), −18.6 (d, ^1J(B,H) = 125 Hz, 2B), −22.6 (2B), −25.1 (d, ^1J(B,H) = 112 Hz, 1B), −31.6 (2B). Anal. Calcd for $C_{39}H_{42}B_9ClP_2RuS_2$: C, 53.80; H, 4.86; S, 7.37. Found: C, 53.68; H, 4.92, S, 7.30.

Synthesis of [RuCl(L6)(PPh_3)$_2$]. To 30 cm^3 of deoxygenated ethanol containing 98 mg (0.329 mmol) of [NMe_4](**L6**) was added [$RuCl_2(PPh_3)_3$] (315 mg, 0.328 mmol), and the mixture was refluxed for 1 h. An orange solid was separated by filtering the warm mixture. The solid was washed with warm ethanol and ethyl ether to yield the analytically pure solid [RuCl(L6)(PPh_3)$_2$], yield 200 mg (69%). FTIR (KBr; ν, cm^{-1}): 2547, 2530 (B–H). ^{1}H FTNMR (400 MHz, $CDCl_3$, 25 °C, TMS; δ): −17.4 (q, 1, Ru*H*), −2.4 (br, 1, B*H*B), 2.77 (d, ^1J = 8.3 Hz, 2, C*H*$_2$), 3.34 (d, ^1J = 8.3 Hz, 2, C*H*$_2$), 7.16–7.37 (m, 30, C_{aryl}–*H*). ^{11}B FTNMR (128 MHz, CH_2Cl_2, 25 °C, $BF_3 \cdot Et_2O$; δ): −5.7 (2B), −16.5 (2B), −19.0 (2B), −29.9 (d, ^1J(B,H) = 106 Hz, 2B), −36.3 (1B). Anal. Calcd for $C_{40}H_{44}B_9ClP_2RuS_2$: C, 54.31; H, 5.01; S, 7.25. Found: C, 53.76; H, 5.00, S, 7.02.

Synthesis of [RuCl(L7)(PPh_3)$_2$]. To 40 cm^3 of deoxygenated ethanol containing 38 mg (0.122 mmol) of [NMe_4](L7) was added [$RuCl_2(PPh_3)_3$] (100 mg, 0.104 mmol), and the mixture was refluxed for 1 h. An orange solid was separated by filtering the warm mixture. The solid was washed with warm ethanol and ethyl ether to yield the analytically pure solid [RuCl(L7)(PPh_3)$_2$], yield 72 mg (77%). FTIR (KBr; ν, cm^{-1}): 2563, 2556, 2533, 2526, 2514 (B–H). ^{1}H FTNMR (400 MHz, $CDCl_3$, 25 °C, TMS; δ): −17.3 (q, 1, Ru*H*), −2.3 (br, 1, B*H*B), 1.85 (m, 1, C*H*$_2$), 2.68 (m, 3, C*H*$_2$, SC*H*$_2$), 3.20 (t, ^1J = 12 Hz, 2, SC*H*$_2$), 7.37–7.14 (m, 30, C_{aryl}–*H*). ^{11}B FTNMR (128 MHz, CH_2Cl_2, 25 °C, $BF_3 \cdot Et_2O$; δ): −6.2 (2B), −17.4 (d, ^1J(B,H) = 130 Hz, 2B), −20.1 (2B), −27.6 (d, ^1J(B,H) = 107 Hz, 1B), −31.8 (d, ^1J(B,H) = 78 Hz, 1B), −36.6 (d, ^1J(B,H) = 138 Hz, 1B). ^{31}P FTNMR (161 MHz, CH_2Cl_2, 25 °C, H_3PO_4; δ): 33.90 (s, *P*Ph_3). Anal. Calcd for $C_{41}H_{46}B_9ClP_2RuS_2$: C, 54.80; H, 5.16; S, 7.14. Found: C, 54.68; H, 5.15; S, 7.09.

Synthesis of [RuCl(L8)(PPh_3)$_2$]·Me_2CO. To 40 cm^3 of deoxygenated ethanol containing 38 mg (0.117 mmol) of [NMe_4](**L8**) was added [$RuCl_2(PPh_3)_3$] (100 mg, 0.104 mmol), and the mixture was refluxed for 1 h. An orange solid was separated by filtering the warm mixture. The solid was washed with warm ethanol. After recrystallization in acetone, 55 mg (58%) of [RuCl(**L8**)(PPh_3)$_2$]·Me_2CO was obtained. FTIR (KBr; ν, cm^{-1}): 2548, 2540 (B–H). ^{1}H FTNMR (400 MHz, $CDCl_3$, 25 °C, TMS; δ): −18.20 (q, 1, Ru*H*), −2.58 (br, 1, B*H*B), 1.71 (m, 2, C*H*$_2$), 2.53 (m, 2, C*H*$_2$), 2.95 (m, 4, C*H*$_2$), 7.40–7.10 (m, 30, C_{aryl}–*H*). ^{11}B FTNMR (128 MHz, CH_2Cl_2, 25 °C, $BF_3 \cdot Et_2O$; δ): −7.5 (2B), −18.0 (4B), −27.6 (d, ^1J(B,H) = 109 Hz, 1B), −32.0 (d, ^1J(B,H) = 100 Hz, 1B), −36.3 (d, ^1J(B,H) = 137 Hz, 1B). Anal. Calcd for $C_{45}H_{54}B_9ClOP_2RuS_2$: C, 55.69; H, 5.61; S, 6.61. Found: C, 55.59; H, 5.59; S, 6.39.

Synthesis of [RuCl(L6)($PMePh_2$)$_2$]. To 40 cm^3 of deoxygenated ethanol containing 30.9 mg (0.104 mmol) of [NMe_4](L6) was added [$RuCl_2(PMePh_2)_4$] (100 mg, 0.104 mmol), and the mixture was refluxed for 1 h. The solvent was then removed, and the residue was treated with 25 cm^3 of dichloromethane and 5 cm^3 of hexane. After filtration, the solution was concentrated slowly and an orange crystalline solid was obtained. The solid was separated by filtration and then washed with hexane, ethanol, and hexane to yield the analytically pure solid [RuCl(L6)($PMePh_2$)$_2$], yield 60 mg (75%). FTIR (KBr; ν, cm^{-1}): 2600, 2548, 2534, 2520 (B–H). ^{1}H FTNMR (400 MHz, $CDCl_3$, 25 °C, TMS; δ): −17.4 (br, 1, Ru*H*), −2.38 (br, 1, B*H*B), 1.60 (m, 6, PC*H*$_3$Ph$_2$), 2.88 (d, ^1J = 7.4 Hz, 2, C*H*$_2$), 3.27 (d, ^1J = 7.4 Hz, 2, C*H*$_2$), 7.65–7.20 (m, 20, C_{aryl}–*H*). ^{11}B FTNMR (128 MHz, CH_2Cl_2, 25 °C, $BF_3 \cdot Et_2O$; δ): −7.5 (2B), −18.3 (d, ^1J(B,H) = 138 Hz, 2B), −21.2 (2B), −31.2 (d, ^1J(B,H) = 107 Hz, 1B), −32.4 (1B), −38.4 (d, ^1J(B,H) = 146 Hz, 1B). ^{31}P FTNMR (161 MHz, CH_2Cl_2, 25 °C, H_3PO_4; δ): 20.00 (s, *P*MePh$_2$). Anal. Calcd for $C_{30}H_{40}B_9ClP_2RuS_2$: C, 47.38; H, 5.30; S, 8.43. Found: C, 47.45; H, 5.38, S, 8.23.

Synthesis of [RuCl(L7)($PMePh_2$)$_2$]. To 40 cm^3 of deoxygenated ethanol containing 32.2 mg (0.103 mmol) of [NMe_4](L7) was added [$RuCl_2(PMePh_2)_4$] (100 mg, 0.103 mmol), and the mixture was refluxed for 1 h. The solvent was then removed, and the residue was treated with 25 cm^3 of dichloromethane and 5 cm^3 of hexane. After filtration, the solution was concentrated slowly and an orange crystalline solid was obtained. The solid was separated by filtration and then washed with hexane, ethanol, and hexane to yield the analytically pure solid [RuCl(L7)($PMePh_2$)$_2$], yield 52 mg (65%). FTIR (KBr; ν, cm^{-1}): 2552, 2517 (B–H). ^{1}H FTNMR (400 MHz, $CDCl_3$, 25 °C, TMS; δ): −17.09 (br, 1, Ru*H*), −2.18 (br, 1, B*H*B), 1.58 (m, 6, PC*H*$_3$Ph$_2$), 1.92 (q, ^1J = 13 Hz, 1, C*H*$_2$), 2.63 (d, ^1J = 13 Hz, 1, C*H*$_2$), 2.82 (m, 2, SC*H*$_2$), 3.08 (t, ^1J = 13 Hz, 2, SC*H*$_2$), 7.60–7.20 (m, 20, C_{aryl}–*H*). ^{11}B FTNMR (128 MHz, CH_2Cl_2, 25 °C, $BF_3 \cdot Et_2O$; δ): −4.9 (2B), −16.0 (d, ^1J(B,H) = 143 Hz, 2B), −18.6 (2B), −25.9 (d, ^1J(B,H) = 103 Hz, 1B), −31.0 (d, ^1J(B,H) = 95 Hz, 1B), −33.5 (d, ^1J(B,H) = 140 Hz, 1B). Anal. Calcd for $C_{31}H_{42}B_9ClP_2RuS_2$: C, 48.07; H, 5.47; S, 8.28. Found: C, 48.22; H, 5.64; S, 8.27.

Synthesis of [NMe_4][$RuCl_2$(Lo)($PMePh_2$)$_2$]. To 18 cm^3 of deoxygenated methanol containing 40.0 mg (0.133 mmol) of [NMe_4](**Lo**) was added [$RuCl_2(PMePh_2)_4$] (102 mg, 0.105 mmol), and the mixture was left at room temperature for 16 h. The resulting yellow solid was filtered and washed with methanol and hexane to yield the analytically pure solid [NMe_4][$RuCl_2$(Lo)($PMePh_2$)$_2$], yield 60 mg (66%). FTIR (KBr; ν, cm^{-1}): 2597, 2542, 2512 (B–H). ^{1}H FTNMR (400 MHz, CD_3COCD_3, 25 °C, TMS; δ): −1.63 (br, 1, B*H*B), 1.43 (m, 6, SC*H*$_3$), 1.98 (s, 6, PC*H*$_3$Ph$_2$), 3.45 (s, 12, N(C*H*$_3$)$_4$), 7.10–7.40, 7.65–7.75 (m, 20, C_{aryl}–*H*). ^{11}B FTNMR (128 MHz, CH_2Cl_2, 25 °C, $BF_3 \cdot Et_2O$; δ): −4.5 (d, ^1J(B,H) = 120 Hz, 2B), −14.5 (1B), −19.0 (d, ^1J(B,H) = 126 Hz, 2B), −25.4 (2B), −32.4 (d, ^1J(B,H) = 147 Hz, 1B), −34.4 (d, ^1J(B,H) = 110 Hz, 1B). ^{31}P FTNMR (161 MHz, Me_2CO, 25 °C, H_3PO_4; δ): 16.42 (s, *P*MePh$_2$). Anal. Calcd for $C_{34}H_{54}B_9Cl_2NP_2RuS_2$: C, 46.82; H, 6.24; N, 1.61; S, 7.35. Found: C, 47.91; H, 6.09; N, 1.40; S, 6.77.

Synthesis of [RuH(L6)(PPh_3)$_2$]. To 30 cm^3 of deoxygenated ethanol containing 64 mg (0.215 mmol) of [NMe_4](L6) was added [Ru(AcO)H(PPh_3)$_3$] (200 mg, 0.211 mmol), and the mixture was refluxed for 1 h. An orange solid was separated by filtering the warm mixture. The solid was washed with boiling ethanol and hexane to yield the analytically pure solid [RuH(L6)(PPh_3)$_2$], yield 140 mg (78%). FTIR (KBr; ν, cm^{-1}): 2596, 2547, 2509 (B–H). ^{1}H FTNMR (400 MHz, $CDCl_3$, 25 °C, TMS; δ): −21.1 (t, ^1J(P,H) = 24 Hz, 1, Ru*H*), −4.3 (br, 1, Ru*H*B), −2.6 (br, 1, B*H*B), 2.75 (d, ^1J = 8.8 Hz, 2, C*H*$_2$), 2.95 (d, ^1J = 8.8 Hz, 2, C*H*$_2$), 6.90–7.70 (m, 30, C_{aryl}–*H*). ^{11}B FTNMR (128 MHz, CH_2Cl_2, 25 °C, $BF_3 \cdot Et_2O$; δ): −9.2 (2B), −19.3 (2B), −21.9 (2B), −24.3 (1B), −32.4 (1B), −38.8 (1B). ^{31}P FTNMR (161 MHz, CH_2Cl_2, H_3PO_4; δ): 56.88 (d, ^1J(P,H) = 22.8 Hz, *P*Ph$_3$). Anal. Calcd for $C_{40}H_{45}B_9P_2RuS_2$: C, 56.51; H, 5.33; S, 7.54. Found: C, 56.61; H, 5.17; S, 6.58.

Synthesis of [RuH(L7)(PPh_3)$_2$]. To 30 cm^3 of deoxygenated ethanol containing 33 mg (0.111 mmol) of [NMe_4](L7) was added [Ru(AcO)H(PPh_3)$_3$] (100 mg, 0.106 mmol), and the mixture was refluxed for 1 h. An orange solid was separated by filtering the warm mixture. The solid was washed with boiling ethanol and hexane to yield the analytically pure solid [RuH(L7)(PPh_3)$_2$], yield 75 mg (83%). FTIR (KBr; ν, cm^{-1}): 2553, 2544 (B–H). ^{1}H FTNMR (400 MHz, $CDCl_3$, 25 °C, TMS; δ): −21.1 (t, ^1J(P,H) = 26 Hz, 1, Ru*H*), −3.42 (br, 1, Ru*H*B), −2.43 (br, 1, B*H*B), 2.29 (m, 4, SC*H*$_2$, C*H*$_2$), 2.57 (m, 2, SC*H*$_2$), 7.10–7.35 (m, 30, C_{aryl}–*H*). ^{11}B

FTNMR (128 MHz, CH_2Cl_2, 25 °C, $BF_3\cdot Et_2O$; δ): −8.8 (2B), −18.9 (d, ^1J(B,H) = 131 Hz, 3B), −21.4 (4B), −33.0 (1B), −36.6 (d, ^1J(B,H) = 145 Hz, 1B). ^{31}P FTNMR (161 MHz, CH_2Cl_2, H_3PO_4; δ): 59.1 (d, ^1J(P,H) = 24 Hz, *P*Ph₃). Anal. Calcd for $C_{41}H_{47}B_9P_2RuS_2$: C, 56.98; H, 5.48; S, 7.42. Found: C, 56.18; H, 5.67; S, 7.23.

Synthesis of [RuH(L8)(PPh₃)₂]. To 30 cm³ of deoxygenated ethanol containing 34.6 mg (0.106 mmol) of [NMe_4](**L8**) was added [Ru(AcO)H(PPh_3)₃] (100 mg, 0.105 mmol), and the mixture was refluxed for 1 h. An orange solid was separated by filtering the warm mixture. The solid was washed with boiling ethanol, methanol, and hexane to yield the analytically pure solid [RuH(L8)(PPh_3)₂], yield 60 mg (65%). FTIR (KBr; ν, cm^{-1}): 2533 (B–H). ^1H FTNMR (400 MHz, $CDCl_3$, 25 °C, TMS; δ): −25.65 (t, ^1J(P,H) = 26.8 Hz, 1, Ru*H*), −2.64 (br, 1, B*H*B), −2.1 (br, 1, B*H*Ru), 1.40 (br, 4, SC*H*₂), 1.92 (br, 2, SC*H*₂), 2.71 (br, 2, SC*H*₂), 7.15–7.70 (m, 30, C_{aryl}–*H*). ^{11}B FTNMR (128 MHz, CH_2Cl_2, 25 °C, $BF_3\cdot Et_2O$; δ): −10.4 (2B), −18.3 (5B), −32.8 (d, ^1J(B,H) = 105 Hz, 1B), −37.1 (d, ^1J(B,H) = 145 Hz, 1B). ^{31}P FTNMR (161 MHz, CH_2Cl_2, H_3PO_4; δ): 57.95 (s, *P*Ph₃). Anal. Calcd for $C_{42}H_{49}B_9P_2RuS_2$: C, 57.57; H, 5.64; S, 7.32. Found: C, 56.58; H, 5.70; S, 6.96.

Synthesis of [RuCl(L6)(Me₂SO)₂]. To 40 cm³ of deoxygenated ethanol containing 61.5 mg (0.207 mmol) of [NMe_4](**L6**) was added [$RuCl_2(Me_2SO)_4$] (100 mg, 0.206 mmol), and the mixture was refluxed for 1 h. The solvent was removed, and the residue was treated with dichloromethane (25 cm³) and hexane (5 cm³). After filtration, the solution was concentrated slowly and an orange crystalline solid was obtained. The solid was separated by filtration and then was washed with hexane, ethanol, and hexane to yield the analytically pure solid [RuCl(L6)(Me_2SO)₂], yield 37 mg (35%). FTIR (KBr; ν, cm^{-1}): 2552, 2529, 2518 (B–H); 1115, 1031, 1018 (S–O). ^1H FTNMR (400 MHz, CD_3COCD_3, 25 °C, TMS; δ): −14.80 (tet, ^1J(B,H) = 106 Hz, 1, br, Ru*H*), −2.21 (br, 1, B*H*B), 2.88 (m, 8, SC*H*₂, (C*H*₃)₂SO), 3.46 (m, 8, SC*H*₂, (C*H*₃)₂SO). ^{11}B FTNMR (128 MHz, Me_2CO, 25 °C, $BF_3\cdot Et_2O$; δ): −6.0 (d, ^1J(B,H) = 138 Hz, 2B), −17.1 (d, ^1J(B,H) = 141 Hz, 2B), −20.9 (d, ^1J(B,H) = 155 Hz, 2B), −30.3 (1B), −31.5 (d, ^1J(B,H) = 111 Hz, 1B), −37.5 (d, ^1J(B,H) = 151 Hz, 1B). Anal. Calcd for $C_8H_{26}B_9ClO_2RuS_4$: C, 18.61; H, 5.08; S, 24.84. Found: C, 18.61; H, 5.12; S, 24.54.

Synthesis of [RuCl(L7)(Me₂SO)₂]. To 40 cm³ of deoxygenated ethanol containing 64.5 mg (0.207 mmol) of [NMe_4](**L7**) was added [$RuCl_2(Me_2SO)_4$] (100 mg, 0.206 mmol), and the mixture was refluxed for 1 h. The solvent was removed, and the residue was treated with dichloromethane (25 cm³) and hexane (5 cm³). After filtration, the solution was concentrated slowly and an orange crystalline solid was obtained. The solid was separated by filtration and then was washed with hexane, ethanol, and hexane to yield the analytically pure solid [RuCl(L7)(Me_2SO)₂], yield 25 mg (23%). FTIR (KBr; ν, cm^{-1}): 2540, 2532 (B–H); 1121, 1101, 1015 (S–O). ^1H FTNMR (400 MHz, CD_3COCD_3, 25 °C, TMS; δ): −14.33 (tet, ^1J(B,H) = 107 Hz, 1, br, Ru*H*), −2.19 (br, 1, B*H*B), 2.09 (s, 2, C*H*₂), 2.79 (s, 1, SC*H*₂), 2.82 (s, 1, SC*H*₂), 3.26, 3.34, 3.29, 3.42, 3.40, 3.46, 3.49 (s, 14, SC*H*₂, (C*H*₃)₂SO). ^{11}B FTNMR (128 MHz, Me_2CO, 25 °C, $BF_3\cdot Et_2O$; δ): −4.2 (d, ^1J(B,H) = 140 Hz, 2B), −15.6 (d, ^1J(B,H) = 143 Hz, 2B), −19.4 (d, ^1J(B,H) = 146 Hz, 2B), −27.5 (d, ^1J(B,H) = 108 Hz, 1B), −29.7 (d, ^1J(B,H) = 114 Hz, 1B), −35.2 (d, ^1J(B,H) = 163 Hz, 1B). Anal. Calcd for $C_9H_{28}B_9ClO_2RuS_4$: C, 20.38; H, 5.32; S, 24.18. Found: C, 20.57; H, 5.56; S, 24.30.

Synthesis of [RuCl(L6)(phenan)]. To 40 cm³ of deoxygenated ethanol containing 60 mg (0.201 mmol) of [NMe_4](**L6**) was added 1,10-phenanthroline hydrate (40 mg, 0.202 mmol) and [$RuCl_2(dmso)_4$] (100 mg, 0.206 mmol), and the mixture was refluxed for 2 h. An orange solid was separated by filtering the warm mixture. The solid was washed with methanol and ethyl ether to yield 26 mg of the analytically pure solid [RuCl(L6)(phenan)]. The solvent was then removed, and the residue was treated with dichloromethane and hexane (25 cm³, 1/1). The solution was concentrated slowly, and 26 mg more of [RuCl(L6)(phenan)] was obtained; total yield 50%. FTIR (KBr; ν, cm^{-1}): 2540 (B–H). ^{11}B FTNMR (128 MHz, CH_2Cl_2, 25 °C, $BF_3\cdot Et_2O$; δ): −6.3 (2B), −17.2 (d, ^1J(B,H) = 146 Hz, 2B), −20.5 (d, ^1J(B,H) = 164 Hz, 2B), −30.4 (1B), −31.5 (d, ^1J(B,H) = 104 Hz, 1B), −37.1 (d, ^1J(B,H) = 150 Hz, 1B). Anal. Calcd for $C_{16}H_{22}B_9ClN_2RuS_2$: C, 35.57; H, 4.10; N, 5.18; S, 11.87. Found: C, 35.40; H, 4.04; N, 4.95; S, 11.93.

Synthesis of [RuCl(L7)(phenan)]. To 40 cm³ of deoxygenated ethanol containing 60 mg (0.192 mmol) of [NMe_4](**L7**) was added 1,10-phenanthroline hydrate (48.5 mg, 0.194 mmol) and [$RuCl_2(dmso)_4$] (95 mg, 0.196 mmol), and the mixture was refluxed for 2 h. An orange solid was separated by filtering the warm mixture. The solid was washed with methanol and ethyl ether to yield 54 mg (52%) of the analytically pure solid [RuCl(L7)(phenan)]. FTIR (KBr; ν, cm^{-1}): 2548, 2526, 2520 (B–H). ^{11}B FTNMR (128 MHz, CH_2Cl_2, 25 °C, $BF_3\cdot Et_2O$; δ): −6.9 (d, ^1J(B,H) = 130 Hz, 2B), −18.2 (d, ^1J(B,H) = 145 Hz, 2B), −21.5 (d, ^1J(B,H) = 153 Hz, 2B), −30.1 (d, ^1J(B,H) = 116 Hz, 1B), −32.3 (1B), −37.4 (d, ^1J(B,H) = 142 Hz, 1B). Anal. Calcd for $C_{17}H_{24}B_9ClN_2RuS_2$: C, 36.83; H, 4.36; N, 5.05; S, 11.56. Found: C, 36.56; H, 4.33; N, 5.16; S, 11.78.

Synthesis of [NMe₄][RuCl(L6)₂]. To 50 cm³ of deoxygenated ethanol containing 300 mg (1.01 mmol) of [NMe_4](**L6**) was added $RuCl_3\cdot xH_2O$ (41.9% Ru; 100 mg, 0.415 mmol), and the mixture was refluxed for 2 h. A green solid was separated by filtering the warm mixture. The solid was washed several times with ethanol/water (1:1) until the solid became orange. Analytically pure crystals of [NMe_4][RuCl(**L6**)₂] suitable for X-ray analysis were grown from acetone; yield 146 mg (57%). FTIR (KBr; ν, cm^{-1}): 2638, 2530 (B–H). ^1H FTNMR (400 MHz, CD_3COCD_3, 25 °C, TMS; δ): −17.5 (tet, ^1J(B,H) = 114 Hz, Ru*H*), −3.02 (br, 1, B*H*B), −2.02 (br, 1, B*H*B), 2.95–3.14 (m, 4, SC*H*₂), 3.20–3.32 (m, 4, SC*H*₂), 3.45 (s, 12, N(C*H*₃)₄). ^{11}B FTNMR (128 MHz, Me_2CO, 25 °C, $BF_3\cdot Et_2O$; δ): −5.9 (d, ^1J(B,H) = 140 Hz, 4B), −7.8 (d, ^1J(B,H) = 123 Hz, 1B), −14.0 (d, ^1J(B,H) = 140 Hz, 2B), −16.6 (d, ^1J(B,H) = 141 Hz, 2B), −19.2 (d, ^1J(B,H) = 154 Hz, 4B), −29.3 (1B), −30.4 (2B), −31.3 (1B), −34.9 (d, ^1J(B,H) = 148 Hz, 1B). Anal. Calcd for $C_{12}H_{40}B_{18}ClNRuS_4$: C, 21.91; H, 6.13; N, 2.13; S, 19.50. Found: C, 22.94; H, 6.23; N, 2.22; S, 19.19.

Synthesis of [NMe₄][RuCl(L7)₂]. To 30 cm³ of deoxygenated ethanol containing 100 mg (0.321 mmol) of [NMe_4](**L7**) was added $RuCl_3\cdot xH_2O$ (41.9% Ru; 38.4 mg, 0.159 mmol), and the mixture was refluxed for 1 h. The green solution was evaporated to dryness and was treated with dichloromethane (25 cm³); the resulting brown solution was filtered, and 5 cm³ of hexane was added. After filtration, the solvent was slowly evaporated, and an orange crystalline solid was obtained; yield 44 mg (40%) of [NMe_4][RuCl(**L7**)₂]. FTIR (KBr; ν, cm^{-1}): 2544, 2531 (B–H). ^1H FTNMR (400 MHz, CD_3COCD_3, 25 °C, TMS; δ): −8.2, −6.2 (br, 1, B*H*Ru), −2.18 (br, 1, B*H*B), 1.88 (m, 2, C*H*₂), 2.72 (m, 2H, C*H*₂), 3.12 (d, ^1J = 12 Hz, 4, SC*H*₂), 3.45 (s, 12, N(C*H*₃)₄), 3.52 (t d, ^1J = 13.0, 3.7 Hz, 4, SC*H*₂). ^{11}B FTNMR (128 MHz, Me_2CO, 25 °C, $BF_3\cdot Et_2O$; δ): −8.3 (d, ^1J(B,H) = 145 Hz, 2B), −16.7 (d, ^1J(B,H) = 143 Hz, 2B), −18.6 (2B), −20.9 (d, ^1J(B,H) = 140 Hz, 1B), −31.5 (d, ^1J(B,H) = 99 Hz, 1B), −36.1 (d, ^1J(B,H) = 143 Hz, 1B). Anal. Calcd for $C_{14}H_{44}B_{18}ClNRuS_4$: C, 24.52; H, 6.47; N, 2.04; S, 18.70. Found: C, 24.60; H, 6.83; N, 2.05; S, 18.79.

X-ray Study of [RuCl(L5)(PPh₃)₂]. The unit cell parameters were determined by least-squares refinement of 25 carefully centered reflections measured on a Nicolet P3F diffractometer. The space group, $P2_1/c$, was confirmed by systematic absences and structure analysis. The structure was solved by the Patterson method[14] and successive Fourier maps. In the final refinements the non-hydrogen atoms were refined anisotropically and the hydrogen atoms isotropically. The final $R(F_o)$ value was 0.058 ($R_w(F_o)$ = 0.041). All refinements were performed using the XTAL2.6 program system,[15] which minimized the function $\sum w(|F_o| - |F_c|)^2$, where $w = 1/\sigma^2(F)$. All calculations were carried out on a VAX 8650 computer.

---

(14) Sheldrick, G. M. SHELXS86: Program for the Solution of Crystal Structures; University of Göttingen: Göttingen, Germany, 1986.

(15) Hall, S. R., Stewart, J. M., Eds. *XTAL2.6 User's Manual*; University of Western Australia, Nedlands, Australia, and University of Maryland: College Park, MD, 1987.

Table 10. Crystallographic Data for $[RuCl(L5)(PPh_3)_2]$, $[RuCl(L8)(PPh_3)_2]\cdot Me_2CO$, and $[NMe_4][RuCl(L6)_2]$

	$[RuCl(L5)(PPh_3)_2]$	$[RuCl(L8)(PPh_3)_2]\cdot Me_2CO$	$[NMe_4][RuCl(L6)_2]$
chem formula	$C_{39}H_{42}B_9ClP_2RuS_2$	$C_{45}H_{54}B_9ClOP_2RuS_2$	$C_{12}H_{40}B_{18}ClNRuS_4$
fw	870.65	970.80	657.84
a (Å)	15.134(3)	12.187(4)	19.423(4)
b (Å)	11.825(3)	17.163(3)	13.028(2)
c (Å)	22.970(4)	12.018(2)	12.142(2)
α (deg)	90.0	95.73(1)	90.0
β (deg)	110.32(2)	95.51(2)	90.0
γ (deg)	90.0	105.61(2)	90.0
V (Å^3)	4111(2)	2389(1)	3073(1)
Z	4	2	4
space group	monoclinic, $P2_1/c$	triclinic, $P\bar{1}$	orthorhombic, $Cmc2_1$
T (°C)	23	23	23
λ (Å)	0.710 69	0.710 69	0.710 69
ρ (g cm^{-3})	1.407	1.349	1.421
μ (cm^{-1})	6.4	5.6	8.5
transmissn coeff	0.98–1.00	0.93–1.00	0.98–1.00
$R(F_o)$	0.058	0.041	0.064
$R_w(F_o)$	0.041	0.046	0.064

X-ray Study of $[NMe_4][RuCl(L6)_2]$. The unit cell parameters were determined by least-squares refinement of 25 carefully centered reflections measured on a Nicolet P3F diffractometer. The structure was solved by direct methods[14] and successive Fourier maps. The space group $Cmc2_1$ was confirmed through absent reflections and structure analysis. The molecule assume m symmetry with the metal and chlorine atoms occupying the mirror plane. The carborane cages are disordered so that the open face is anti or syn with regard to the metal, and thus, the B(3) atom occupies two positions, both assuming a population parameter of 0.5. In the final refinements the disordered B(3) atom and the carbon atoms C(21)–C(23) of the NMe_4 group were refined with isotropic thermal parameters and the rest of the non-hydrogen atoms with anisotropic thermal parameters. Of the hydrogen atoms, only those bonded to carbon atoms C(1) and C(2) were included in the calculations in fixed positions (C–H = 0.95 Å and U = 0.05 Å^2). The final $R(F_o)$ value was 0.064 ($R_w(F_o)$ = 0.064). Refinement of the enantiomeric model did not decrease the R factor ($R(F)$ = 0.064 and $R_w(F_o)$ = 0.065). All refinements were performed using the XTAL2.6 program system,[15] which minimized the function $\sum w(|F_o| - |F_c|)^2$, where $w = 1/\sigma^2(F)$. All calculations were carried out on a VAX 8650 computer.

X-ray Study of $[RuCl(L8)(PPh_3)_2]\cdot Me_2CO$. Single-crystal data collection was performed at 296(1) K with a Rigaku AFC5S diffractometer using monochromatized Mo Kα radiation (λ = 0.710 96 Å). The unit cell parameters were determined by least-squares refinement of 25 carefully centered reflections (36° < 2θ < 40°). The data obtained were corrected for Lorentz and polarization effects and for dispersion. Also, a correction for empirical absorption (ψ scan) was applied. A total of 11 490 reflections were collected by the $\omega/2\theta$ scan mode ($2\theta_{max}$ = 50°), giving 10 969 unique reflections (R_{int} = 0.016). Of those, 8250 were considered as observed according to the criterion $I > 2\sigma(I)$. The 3 check reflections monitored after every 150 reflections showed only statical fluctuations during the course of the data collection. The structure was solved by direct methods using MITHRIL.[16] Least-squares refinements and all subsequent calculations were performed using the TEXSAN[17] crystallographic software package, which minimized the function $\sum w(|F_o| - |F_c|)^2$, where $w = 1/\sigma^2(F)$. The acetone molecule was disordered, as was the C(2) atom in the C(1)–C(2)–C(3)–C(4) chain. Refinement of the non-hydrogen atoms with anisotropic temperature factors, except the atoms of the acetone molecule and disordered C(2) atoms (isotropic factors) and of the BH hydrogen atoms with fixed isotropic temperature parameters and of the phenyl and CH_2 hydrogen atoms (only H2a) by inclusion in calculated positions with fixed isotropic temperature factors reduced the R value to 0.041 (R_w = 0.046) for 567 parameters. Neutral atomic scattering factors were those included in the program. Structures were plotted with ORTEP.[18]

Acknowledgment. This work was supported by a grant from the Spanish Government (No. PB87-0364, CICYT, Spain). R.K. is grateful to Oskar Öflunds Stiftelse and Suomen Kulttuurirahasto for financial support. We thank Bruker (Dr. Bourdonneau) for running HETCOR spectra.

Supplementary Material Available: Tables of positional parameters, thermal parameters, bond distances and angles, and least-squares planes (22 pages). Ordering information is given on any current masthead page.

OM940074H

---

[16] Gilmore, C. J. *J. Appl. Crystallogr.* **1982**, *17*, 42.

[17] TEXSAN-TEXRAY: Single Crystal Structure Analysis Package, Version 5.0; Molecular Structure Corp.: The Woodlands, TX, 1989.

[18] Johnson, C. K. ORTEP-II; Report ORNL-5138; Oak Ridge National Laboratory: Oak Ridge, TN, 1976.

[19] The w angle is defined as the dihedral angle between the planes S–C_c–C_c–S and S–M–S (C_c = carbon atom of the boron cage).